ChemComm

COMMUNICATION

View Article Online
View Journal

Cite this: DOI: 10.1039/d1cc00343g

Received 20th January 2021,
Accepted 23rd April 2021

DOI: 10.1039/d1cc00343g

rsc.li/chemcomm

A GLUT1 inhibitor-based probe significantly ameliorates the sensitivity of tumor detection and diagnostic imaging†

Shengnan Liu, *[a] Weijie Song,[ab] Yujun Cui,[ac] Ziru Sun,[ad] Zhenhua Huang[a] and Qingzhi Gao *[a]

We report a non-antibody GLUT1 inhibitor probe NBDQ that is 30 times more sensitive than the traditional GLUT1 transportable tracer for cancer cell imaging and Warburg effect-based tumor detection. NBDQ reveals significant advantages in terms of tumor selectivity, fluorescence stability and *in vivo* biocompatibility in xenograft tumor imaging, including triple-negative breast cancer.

The Warburg effect has been consistently recognized in cancers through increased rates of glucose transport and metabolism. Targeting this elevated glycolysis or overexpressed GLUTs has provided a promising therapeutic strategy, which has been a key catalyst for targeted therapeutic cancer drug development and clinical diagnostic tumor imaging.[1] ^{18}F-FDG-PET (2-[^{18}F]-fluoro-2-deoxy-D-glucose based positron emission tomography) is currently the most commonly used clinical modality for tumor diagnosis, cancer staging and recurrence monitoring.[2] Although FDG-PET has revolutionized cancer diagnosis, the use of ^{18}F-FDG still has many disadvantages aside from the technical and logistical problems associated with radioactivity, including high cost, very short half-life (~110 min) that needs to be treated as a perishable substance and is only applicable for immediate evaluation, and particularly the need of fasting for the plasma glucose control.[3] All these disadvantages led efforts to develop non-isotopic bioprobes. The most widely used fluorescent GLUT substrate is 2-[*N*-(7-nitrobenz-2-oxa-1,3-diazol-4-yl)amino]-2-deoxyglucose (2-NBDG), which is designed by installing a structurally compact green fluorophore, NBD (nitrobenzoxadiazole), at the C-2 position of glucosamine (Scheme 1).[4] 2-NBDG can be transported by GLUT1 and produce short-lived, fluorescent 2-NBDG-6-phosphate in high GLUT1-expressing cells[5] and has proven to be useful for *in vitro* glucose uptake monitoring in many different types of GLUT1 overexpressing cancer cells.[6] However, similar to the other transportable glucose tracers, the application of 2-NBDG in tumor labeling has been reported to have several downfalls, including high treatment dosage, low signal intensity due to the intracellular metabolism induced fluorescence decay, and low *in vivo* biocompatibility by competitive physiological glucose inhibition and impairment.[7]

To overcome these challenges, in this work, we propose and demonstrate a novel strategy by employing a fluorescently labeled GLUT1 inhibitor: NBDQ, as a new class of tumor diagnostic agent for more efficient detection and monitoring of Warburg effect-activated glycolysis. NBDQ was derived from the natural flavonoid quercetin through a simple regioselective Mannich coupling with the fluorophore NBD (Scheme 1).

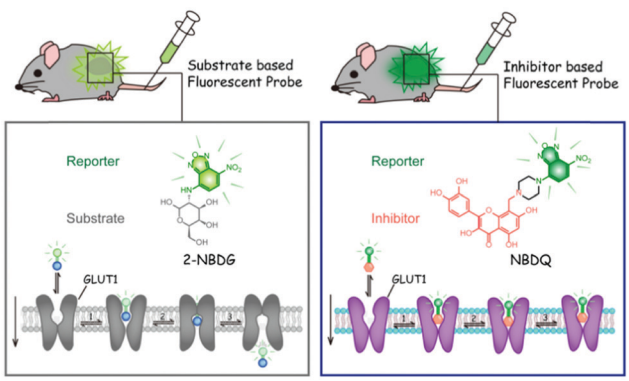

Scheme 1 Design concept of the Warburg effect targeted GLUT1 inhibitor bioprobe. **2-NBDG**: the well-known GLUT1 transportable fluorescent tracer for glucose uptake assessment; **NBDQ**: the newly designed GLUT1 inhibitor bioprobe based on the natural flavonoid quercetin in this study.

[a] *Institute of Molecular Plus, Tianjin Key Laboratory for Modern Drug Delivery & High-Efficiency, School of Pharmaceutical Science and Technology, Tianjin University, 92 Weijin Rd, Nankai, Tianjin 300072, P. R. China. E-mail: shengnan_liu@tju.edu.cn, qingzhi@tju.edu.cn*

[b] *Tianjin Medical University Cancer Institute and Hospital, National Clinical Research Center for Cancer, West Huanhu Road, Hexi, Tianjin 300060, P. R. China Transplantation Center, Tianjin First Central Hospital, 24 Fukang Road, Nankai, Tianjin 300192, P. R. China*

[d] *Department of Biology, Gudui BioPharma Technology Inc., 5 Lanyuan Road, Huayuan Industrial Park, Tianjin 300384, P. R. China*

† Electronic supplementary information (ESI) available. See DOI: 10.1039/d1cc00343g

We revealed that NBDQ deserves a particular merit for more effective Warburg effect based cancer cell detection and significantly improves the *in vivo* tumor diagnostic imaging. Our study reveals the first inhibitor-based approach on non-antibody mediated molecular imaging of GLUT1 overexpression.

Several classes of GLUT inhibitors were identified and synthesized by scientists during their approaches for either diabetes management studies or cancer drug research. Namely, the natural flavonoids, including quercetin, phloretin, phlorizin,[8] the Greek cytos relaxation molecule cytochalasin B,[9] and the natural compound forskolin which is isolated from the plant *Coleus forskohlii*, were frequently used as SGLTs (sodium dependent glucose transporters) and GLUT inhibitors.[10] In addition to the natural compounds, artificially synthesized GLUT1 inhibitor molecules and GLUT targeting nanoparticles have also been extensively pursued for potential targeted drug delivery and biomedical diagnosis.[11] In order to make an optical analog that can be a potent GLUT1 inhibitor, we chose the natural flavonoid quercetin, which is abundant in onions, green tea, and other flavonoids and polyphenol containing plants, as a template for fluorescent derivatization. Quercetin has been found to strongly inhibit glucose transport and intracellular uptake in several cancer cells. The inhibitory effect of quercetin on glucose uptake was established by impairing the Warburg effect, and most importantly, the glucose inhibition of quercetin was confirmed to be independent of extracellular glucose.[12] Based on these observations, NBDQ was designed and synthesized by combining quercetin with the fluorophore of NBD to target the tumor specific Warburg effect.

The preparation details and analytical data of NBDQ are described in the ESI† (Scheme S1 and Fig. S1–S4). In PBS, NBDQ exhibits a minor excitation peak at 343 nm and a major excitation peak at 478 nm, with a single emission at 561 nm (Fig. 1A). The two excitation peaks presumably reflect two distinct states: protonated and unprotonated NBD fluorophores. This unique excitation characteristic makes the probe reach an extremely large Stokes shift (up to 218 nm) and more potentially useful in different biological environments as one may alternate excitation wavelength to avoid potential incompatible cross disturbance with other fluorescent labeling (*e.g.* GFP excitation at ~480 nm). The emission spectrum of NBDQ at 561 nm also gives this probe the potential to perform biological studies regarding the single-molecule fluorescence resonance energy transfer (FRET) mediated spatial resolution. The fluorophores that can be excited by the emission light of NBDQ in terms of a single molecule, as studied by FRET analysis, include Cy3 (excitation at ~530 nm), dsRed1 (excitation at ~560 nm) and rhodamine (excitation at ~543 nm) (Fig. 1A; for more information including excitation and UV–vis spectra, see Fig. S5 and S6, ESI†).

As reported previously,[13] for the uptake of glucose tracer 2-NBDG, increased extracellular concentrations of the probe can lead to increased intracellular probe transport in the GLUT1 overexpressing A549 cancer cells (Fig. 1B, C and Fig. S7A, ESI†). However, a very high concentration of

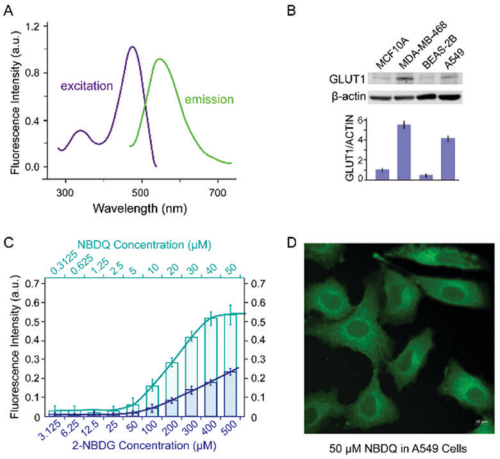

Fig. 1 (A) Fluorescence excitation and emission spectra of NBDQ (50 μM of NBDQ in PBS). (B) The expression level of GLUT1 in MCF10A, MDA-MB-468, BEAS-2B, and A549 cells. (C) The sensitivity in live-cell imaging of NBDQ (0.3–50 μM) and 2-NBDG (3–500 μM) in A549 cells under physiological conditions for 1 h. (D) The fluorescence microscopic imaging of 50 μM of NBDQ labeled A549 cells at 3 h (see Fig. S7B, ESI† for 2-NBDG).

2-NBDG (up to 500 μM) was needed for achieving an acceptable signal-to-noise ratio under physiological cell culture conditions. In the same cell line, the inhibitor probe NBDQ shows a significant improvement for live-cell imaging. Under normal cell culture conditions, 10 μM of NBDQ can achieve the same labeling effect as 300 μM of 2-NBDG (Fig. 1C). The metabolic deterioration of both probes was also remarkably different. For instance, a rapid fluorescence quenching within 3 h was observed in the 2-NBDG (500 μM) treated A549 cells (Fig. S1D, ESI†), whereas the fluorescence of the NBDQ (50 μM) treated cells were found to be stable (Fig. 1D). Thus, with the rationally designed NBDQ, 10 times lower concentration of the probe can realize a 3-fold higher fluorescence intensity and the fluorescence lifetime in living cells was greatly improved. This result demonstrates that NBDQ enables significant improvement in the cancer cell labeling sensitivity and bio- and physiological compatibility over 2-NBDG.

The relationship between GLUT1 expression and cytotoxicity induced by the probe was confirmed using two pairs of normal and neoplastic cell lines, namely, the normal bronchial epithelial BEAS-2B cells and the corresponding human non-small-cell lung cancer A549 cells and non-tumorigenic human breast MCF10A cells and the corresponding human triple-negative breast cancer (TNBC) MDA-MB-468 cells. NBDQ showed low toxicity against the normal BEAS-2B and MCF-10A cells but more toxicity against the GLUT1 high expressing A549 and TNBC cells (Fig. S8, ESI†). This result can be explained by the fact that the specific inhibition of GLUT1 may cause more decreased glucose supply and disturbance to the glycolytic influx in both A549 and TNBC cells.

The GLUT1 specificity and inhibitory effect were confirmed by the 2-DG uptake assay using human red blood cells as an established system because human erythrocytes express GLUT1 as their sole glucose transporter.[14] The known GLUT1 inhibitors, quercetin, phloretin, and CB (Fig. S9A, ESI†), were used to determine the effectiveness and magnitude of NBDQ on the

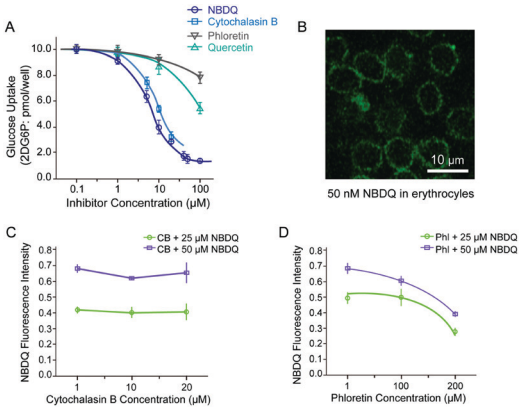

Fig. 2 (A) 2-DG uptake inhibition curves in human erythrocytes with different GLUT1 inhibitors. (B) The confocal fluorescence microscopy imaging of human erythrocytes treated with 50 nM of NBDQ at 37 °C incubated for 30 min. (C) The competitive effect of cytochalasin B (1–20 μM) on NBDQ cellular binding in MDA-MB-468 cells. (D) The competitive effect of phloretin (1–200 μM) on NBDQ cellular binding in MDA-MB-468 cells. Data are presented as mean ± S.E.M.

GLUT1 inhibition. According to the half maximal inhibitory concentrations (IC_{50}, NBDQ: 7.6 ± 1.3 μM; CB: 10.9 ± 2.1 μM; quercetin: 112.0 ± 8.1 μM; phloretin: >200 μM) (Fig. 2A), the GLUT1 inhibition effect of NBDQ is much stronger than that of quercetin and phloretin but similar to the GLUT1 specific inhibitor CB, which reduces the 2-DG uptake in erythrocytes to 52.0 ± 2.3% under 10 μM.

The confocal-laser scanning analysis with 30 min of incubation in human erythrocytes using NBDQ (50 nM) and 2-NBDG (500 nM) has further clarified the differences between these two probes (Fig. 2B and Fig. S9B, ESI†). Under the testing conditions, the intracellularly transported 2-NBDG and surface binding of NBDQ were clearly visualized. To decipher the inhibition mechanism, the competitive inhibitor binding test was carried out by combining CB and phloretin with NBDQ, respectively. In the GLUT1 highly overexpressing MDA-MB-468 cells, the pretreatment of 20 μM of CB did not cause fluorescence intensity changes of NBDQ, whereas an increased amount of phloretin significantly attenuated NBDQ cellular binding (Fig. 2C and D). These results suggest that the GLUT1 inhibition mechanism of NBDQ is different from that of CB, whereas phloretin may share similar binding determinants with NBDQ. The competitive inhibition results on the 2-DG uptake using human erythrocytes revealed the same findings: the pretreatment of a high concentration of phloretin (200 μM) results in no further inhibition of NBDQ on the intracellular uptake of 2-DG but CB (10 μM) treated erythrocytes showed a synergistic inhibitory effect with NBDQ (Fig. S10, ESI†). The kinetic effects of both cytochalasin B and phloretin on glucose transport mediated by GLUT1 are well known. Cytochalasin B acts as a competitive inhibitor of glucose transport out of cells by molecular binding to a site accessible from the endofacial surface of the transporter, whereas phloretin acts as a competitive inhibitor of glucose uptake into cells by binding with a glucose competitive external site.[9,15] These results suggest that NBDQ inhibits glucose transport in a similar fashion to phloretin by interacting with GLUT1 at a specific site close to the exofacial surface of the transporter. The inhibitor binding site and molecular binding mode of NBDQ with GLUT1 were further confirmed by a 150 ns molecular dynamics simulation study with the YASARA program (Fig. S11–S14 and Tables S1–S3, ESI†).

To demonstrate the specificity of NBDQ towards the GLUT1 overexpressing cancer cells, we conducted a simple flow cytometry-based detection and quantification test by using GLUT1 low- and high-expressing BEAS-2B and A549 cells. As an optimal condition, 50 μM of NBDQ with 30 min of incubation was confirmed to allow specific identification of A549 cells according to the GLUT1 expression magnitude (Fig. S15A–C, ESI†). Furthermore, in a spiked mixture, the NBDQ labeling was validated to be able to differentiate cancer cells (A549) from normal cells (BEAS-2B) with a very high sensitivity and excellent accuracy (Fig. S15D and E, ESI†).

To validate the robustness of the probe for *in vivo* diagnostic imaging, we performed an application study of NBDQ in both human TNBC and A549-derived xenograft tumor detection. TNBC diagnostic imaging remains an unmet need due to the lack of representing biomarkers (*i.e.* no estrogen receptor, progesterone receptor and human epidermal growth factor receptor-2).[16] However, a high tumoral glucose uptake regulated by the Warburg effect has been fundamentally recognized as a hallmark and promising target of TNBC for diagnostic imaging and even prognostic staging.[17] Equimolar concentrations of both NBDQ and 2-NBDG were administered by tail vein injection and the mice were imaged after certain time intervals using the Xenogen IVIS *in vivo* imaging system. All animal experiments were approved by the Institutional Animal Ethics Committee and complied with the current guidelines for treating lab animals of China.

As shown in Fig. 3A, the fluorescence signals of NBDQ were clearly differentiated from the surrounding tissues 6 h post a single dose injection. The fluorescence intensity of NBDQ gradually increased and accumulated at the tumor site, indicating that NBDQ could be preferentially recognized and recruited by elevated glycolysis of the TNBC cells (Fig. 3B). The comparison results between NBDQ and equimolar concentration of 2-NBDG revealed that the fluorescence signal of NBDQ considerably outlasted up to 72 h, while the detectable fluorescence intensity for 2-NBDG can only persist for about 12 h post treatment (Fig. 3A *vs.* C). The *ex vivo* optical images and the corresponding probe activities of the main organs from animals sacrificed at 72 h for NBDQ and at 24 h for 2-NBDG are shown in Fig. 3A, C and D. As summarized in Table S4 (ESI†), the highest imaging contrast indicated as tumor-to-background ratio (Tm/Bkg) for NBDQ approaches 12.37 : 1, which is significantly higher than the GLUT1 substrate tracer 2-NBDG (5.44 : 1, Table S4, ESI†). The clinically proved ^{18}F-FDG/PET imaging has been reported to be utilized in the same MDA-MB-468 xenograft mice, but under fasted conditions, and the Tm/Bkg ratio was recorded as 3.21 : 1, which is much lower than NBDQ.[17] The tumor-to-organ ratio (Tm/Torg) of NBDQ for groups of mice was recorded as 8.60 : 1 *versus* 3.48 : 1 for 2-NBDG (n = 3), which is also significantly improved (Fig. 3D and Table S4; see Fig. S16, ESI† and Table S5 for the A549 xenograft imaging study).

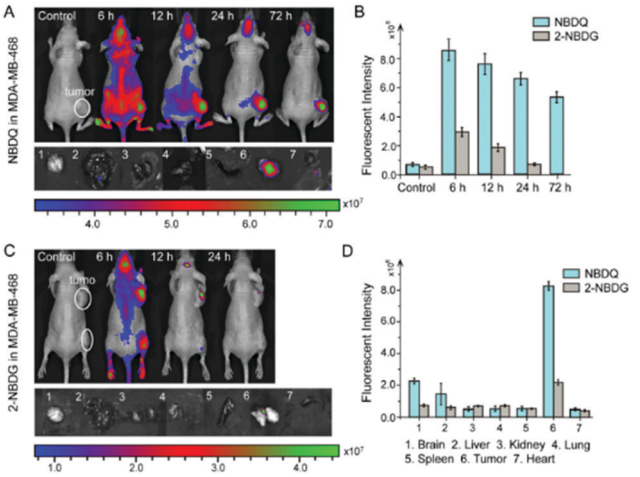

Fig. 3 (A) *In vivo* and *ex vivo* optical images for the NBDQ treated TNBC xenograft mice. Up to 72 h following administration of 0.2 μmol mouse^{-1} of the probe under *ad libitum* feeding conditions. The white circle indicates the location of the tumor. (B) The quantitative analysis of mean fluorescence intensity for both NBDQ and 2-NBDG determined over time by the measurement of respective tumor regions of interest (averaged from n = 3). (C) The 2-NBDG treated TNBC xenograft mice and the *ex vivo* optical images of organs for up to 24 h following the single dose treatment of 0.2 μmol mouse^{-1} under *ad libitum* feeding conditions. (D) The *ex vivo* quantitative bio-distribution from NBDQ (at 72 h) and 2-NBDG (at 24 h) treated mice. Tumors on the forelimb site for 2-NBDG were chosen for the quantitative analysis. λ_{ex}. 470 ± 10 nm and λ_{em}. 565 ± 20 nm.

A primary survey of the potential antitumor efficacy was also carried out with the same TNBC xenograft mice, and the results showed that a daily i.v. treatment of 10 mg kg^{-1} of NBDQ for 6 days revealed about 35% tumor growth suppression (Fig. S17, ESI†).

In conclusion, we have developed a fluorescent GLUT1 inhibitor NBDQ as an optical probe for efficient tumor detection and diagnostic imaging. NBDQ shows clear advantages over transportable glucose tracer 2-NBDG, including desirable tumor-to-normal tissue contrast and excellent tumor selectivity (Tm/Bkg and Tm/Torg), high fluorescence stability (long response time), and ideal physiological biocompatibility. The study provides the first example, to our knowledge, of visualizing the GLUT1 expression with a non-antibody small molecule inhibitor. The characteristics of NBDQ offer the potential promise of the inhibitor probe as an emerging *in vitro* and *in vivo* diagnostic tool for pre- and clinical diagnosis of GLUT1 over-expressing tumors. This is particularly relevant for TNBC, which remains a highly metastatic and lethal disease with a need for specific diagnostics to obtain precise identification.

This study was supported by the National Natural Science Foundation of China (No. 21772144) and the National Key Research & Development (R&D) Program of China (2020YFA0907903).

Conflicts of interest

There are no conflicts to declare.

Notes and references

1 (*a*) O. Warburg, *Science*, 1956, **123**, 309; (*b*) Y. Shi, S. Liu, S. Ahmad and Q. Gao, *Curr. Top. Med. Chem.*, 2018, **18**, 454; (*c*) K. K. S. Sai, A. Zachar, P. M. Bingham and A. Mintz, *Am. J. Roentgenol.*, 2017, **209**, 270; (*d*) M. G. V. Heiden, L. C. Cantley and C. B. Thompson, *Science*, 2009, **324**, 1029.
2 L. C. Ong, Y. Jin, I. C. Song, S. Yu and K. Zhang, *et al.*, *Acta Radiol.*, 2008, **49**, 1145–1153.
3 (*a*) S. Vaidyanathan, C. N. Patel, A. F. Scarsbrook and F. U. Chowdhury, *Clin. Radiol.*, 2015, **70**, 787–800; (*b*) M. B. Lobrano and P. Singha, *Clin. J. Oncol. Nurs.*, 2003, **7**, 379–385; (*c*) R. L. Wahl, C. A. Henry and S. P. Ethier, *Radiology*, 1992, **183**, 643–647.
4 K. Yoshioka, H. Takahashi, T. Homma, M. Saito, K. B. Oh, Y. Nemoto and H. Matsuoka, *Biochim. Biophys. Acta*, 1996, **1289**, 5.
5 K. Yoshioka, M. Saito, K. B. Oh, Y. Nemoto, H. Matsuoka, M. Natsume and H. Abe, *Biosci., Biotechnol., Biochem.*, 1996, **60**, 1899.
6 (*a*) N. Rajaram, A. E. Frees, A. N. Fontanella, J. Zhong, K. Hansen, M. W. Dewhirst and N. Ramanujam, *PLoS One*, 2013, **8**, e76524; (*b*) R. G. O'Neil, L. Wu and N. Mullani, *Mol. Imaging Biol.*, 2005, **7**, 388; (*c*) N. Rouach, A. Koulakoff, V. Abudara, K. Willecke and C. Giaume, *Science*, 2008, **322**, 1551; (*d*) A. Hellebust and R. Richards-Kortum, *Nanomedicine*, 2012, **7**, 429; (*e*) W. H. Kim, J. Lee, D. W. Jung and D. R. Williams, *Sensors*, 2012, **12**, 5005.
7 (*a*) R. A. Sheth, L. Josephson and U. Mahmood, *J. Biomed. Opt.*, 2009, **14**, 064014; (*b*) N. Nitin, A. L. Carlson, T. Muldoon, A. K. El-Naggar, A. Gillenwater and R. Richards-Kortum, *Int. J. Cancer*, 2009, **124**, 2634; (*c*) H. Y. Lee, J. J. Lee, J. Park and S. B. Park, *Chem. – Eur. J.*, 2011, **17**, 143.
8 (*a*) H. J. Martin, F. Kornmann and G. F. Fuhrmann, *Chem.-Biol. Interact.*, 2003, **146**, 225; (*b*) K. E. Hamilton, J. F. Rekman, L. K. Gunnink, B. M. Busscher, J. L. Scott, A. M. Tidball, N. R. Stehouwer, G. N. Johnecheck, B. D. Looyenga and L. L. Louters, *Biochimie*, 2018, **151**, 107; (*c*) A. Pérez, P. Ojeda, L. Ojeda, M. Salas, C. I. Rivas, J. C. Vera and A. M. Reyes, *Biochemistry*, 2011, **50**, 8834.
9 A. Carruthers and A. L. Helgerson, *Biochemistry*, 1991, **30**, 3907.
10 S. Sergeant and H. D. Kim, *J. Biol. Chem.*, 1985, **260**, 14677.
11 (*a*) D. A. Chan, P. D. Sutphin, P. Nguyen, S. Turcotte, E. W. Lai, A. Banh, G. E. Reynolds, J. T. Chi, J. Wu, D. E. Solow-Cordero, M. Bonnet, J. U. Flanagan, D. M. Bouley, E. E. Graves, W. A. Denny, M. P. Hay and A. J. Giaccia, *Sci. Transl. Med.*, 2011, **3**, 94ra70; (*b*) Y. Liu, Y. Cao, W. Zhang, S. Bergmeier, Y. Qian, H. Akbar, R. Colvin, J. Ding, L. Tong, S. Wu, J. Hines and X. Chen, *Mol. Cancer Ther.*, 2012, **118**, 1672; (*c*) H. Siebeneicher, A. Cleve, H. Rehwinkel, R. Neuhaus, I. Heisler, T. Muller, M. Bauser and B. Buchmann, *ChemMedChem*, 2016, **11**, 2261; (*d*) S. Singh, *Colloids Surf., B*, 2017, **155**, 25.
12 L. Moreira, I. Araújo, T. Costa, A. Correia-Branco, A. Faria, F. Martel and E. Keating, *Exp. Cell Res.*, 2013, **319**, 1784.
13 C. Zou, Y. Wang and Z. Shen, *J. Biochem. Biophys. Methods*, 2005, **64**, 207.
14 (*a*) M. Mueckler, C. Caruso, S. A. Baldwin, I. Blench, H. R. Morris, W. J. Allard, G. E. Lienhard and H. F. Lodish, *Science*, 1985, **229**, 941; (*b*) A. Montel-Hagen, S. Kinet, N. Manel, C. Mongellaz, R. Prohaska, J. L. Battini, J. Delaunay, M. Sitbon and N. Taylor, *Cell*, 2008, **132**, 1039; (*c*) A. L. Helgerson and A. Carruthers, *J. Biol. Chem.*, 1987, **262**, 5464; (*d*) S. M. Jarvis, *Biochem. J.*, 1988, **249**, 383; (*e*) A. M. Reyes, F. Bustamante, C. I. Rivas, M. Ortega, C. Donnet, J. P. Rossi, J. Fischbarg and J. C. Vera, *Biochemistry*, 2002, **41**, 8075.
15 (*a*) X. Fu, G. Zhang, R. Liu, J. Wei, D. Zhang-Negrerie, X. Jian and Q. Gao, *J. Chem. Inf. Model.*, 2016, **56**, 517; (*b*) P. Ojeda, A. Pérez, L. Ojeda, M. Vargas-Uribe, C. I. Rivas, M. Salas, J. C. Vera and A. M. Reyes, *Am. J. Physiol.: Cell Physiol.*, 2012, **303**, C530.
16 B. E. Dogan and L. W. Turnbull, *Ann. Oncol.*, 2012, **23**, 23.
17 R. K. Tekade and X. Sun, *Drug Discovery Today*, 2017, **22**, 1637.

